INSTITUTE OF PHYSICS PUBLISHING NANOTECHNOLOGY
Nanotechnology **17** (2006) 4689–4694 doi:10.1088/0957-4484/17/18/027

Synthesis of highly faceted multiply twinned gold nanocrystals stabilized by polyoxometalates

Junhua Yuan[1,2], Yuanxian Chen[1,3], Dongxue Han[1], Yuanjian Zhang[1], Yanfei Shen[1], Zhijuan Wang[1] and Li Niu[1,4]

[1] State Key Laboratory of Electroanalytical Chemistry, Changchun Institute of Applied Chemistry, Graduate School of the Chinese Academy of Sciences, Chinese Academy of Sciences, Changchun 130022, People's Republic of China
[2] Department of Pharmaceutics, Xianning College, Xianning 437100, People's Republic of China
[3] Department of Materials Science, Jilin University, Changchun 130021, People's Republic of China

E-mail: lniu@ciac.jl.cn

Received 21 June 2006, in final form 8 August 2006
Published 30 August 2006
Online at stacks.iop.org/Nano/17/4689

Abstract
A novel and facile chemical synthesis of highly faceted multiply twinned gold nanocrystals is reported. The gold nanocrystals are hexagonal in transmission electron microscopy and icosahedral in scanning electron microscopy. Phosphotungstic acid (PTA), which was previously reduced, serves as a reductant and stabilizer for the synthesis of gold nanocrystals. The PTA–gold nanocomposites are quite stable in aqueous solutions, and electrochemically active towards the hydrogen evolution reaction.

(Some figures in this article are in colour only in the electronic version)

1. Introduction

Recently, nanocomposites have been the focus of basic research and practical use in the field of bio-analysis [1–3], photoelectric devices [4], catalytic application [5, 6] and medical diagnosis and treatment [7–9]. This interest has resulted in the development of numerous protocols for the synthesis of nanostructured materials over a range of sizes. It is now known that besides nanoparticle size and composition, particle shape could be a critical role in their application, notably in modulating their optical and catalytic properties [10, 11]. Gold nanocrystals with various shapes (spheres, rods, wires, prisms, multipods and plates) have been reported. For instance, gold nanorods [12] have been synthesized by electrochemical reduction, gold nanoprisms [13] and gold multipod nanocrystals [14] have been prepared *via* a seed-growth approach, and gold nanoplates [15] have been made by a wet chemical route based on the reduction of a gold precursor with ortho-phenylenediamine. However, there are still only a few reports on highly faceted multiply twinned gold nanocrystals [16–21], such as cubes, tetrahedrons, octahedrons and decahedrons, especially icosahedral Au nanostructures.

Polyoxometalates are well-defined metal-oxide polyanions that can undergo stepwise and multi-electron reactions whilst retaining structural integrity [22]. Noble metal–polyoxometalate nanocomposites [23–26] have been reported, and they exhibit high catalytic activity and selectivity in organic catalysis. The synthesis of the noble metal–polyoxometalates based on photocatalytic reduction has been pioneered by Papaconstantinou *et al* [27]. In the reactions, silicotungstic acid served as the photocatalyst and stabilizer. The as-prepared Au nanoparticles were nearly spherical with a size distribution of 5–20 nm. A strategy for synthesis of noble metal–polyoxometalate nanocomposites was developed by Sastry *et al* [28]. The method produced multiply twinned gold nanoparticles and gold–silver bimetallic nanoparticles with irregular morphology. Thus, it is necessary to exploit a novel protocol for the controlled synthesis of highly faceted multiply twinned noble metal–polyoxometalate nanocomposites with a well-refined shape.

[4] Author to whom any correspondence should be addressed.

Herein we report the one-pot synthesis of gold nanocrystals in the presence of phosphotungstic acid (PTA). The PTA was reduced previously, and then it turned the gold precursors into gold nanocrystals. The as-prepared gold nanocrystals are well-refined, highly faceted and multiply twinned, with a hexagonal shape in transmission electron microscopy (TEM), and an icosahedral shape in scanning electron microscopy (SEM). The novel gold–PTA nanocomposites show a high electrochemical activity towards the hydrogen evolution reaction (HER).

2. Experimental section

2.1. Chemicals

PTA ($H_3PW_{12}O_{40}\cdot 12H_2O$), $HAuCl_4\cdot 4H_2O$ and L-ascorbic acid ($C_6H_8O_6$) were obtained from Aldrich. All reagents were of analytical grade, and the solutions were prepared with deionized water from a Millipore system (18 MΩ).

2.2. Synthesis of highly faceted Au nanoparticles

In a typical synthesis, a 20 ml volume of 1.2 mM $HAuCl_4$ aqueous solution was vigorously stirred and boiled at 100 °C. Simultaneously, equivalent volume (5 ml) solutions of freshly prepared L-ascorbic acid (0.01 M) and PTA (0.02 M) were mixed. To this mixture, a 200 μl volume of 1 M NaOH was added to adjust, until the pH value of the mixture achieved 5–6 and the mixture became deep blue from colourless. Then the mixture was quickly injected into the boiled $HAuCl_4$ solution and it turned from light yellow into wine red. The solution was stirred for 4 h to ensure that the reaction had been completed. The gold colloid was collected by centrifugation at a rate of 8000 rpm for 10 min, redispersed into deionized water and then dialysed to remove uncoordinated PTA in the deionized water for 2 days in a 12 K cutoff dialysis bag (Millipore). The dialysed solution was extremely stable for a month.

2.3. Characterizations of Au nanoparticles

The UV–vis spectra of the dialysed gold colloid solution were collected on a CARY 500 Scan UV/vis/near IR spectrophotometer.

A drop of the dialysed gold colloid solution was put on a carbon–copper grid, and recorded on a JEOL 2000 TEM operating at 200 kV. 20 μl of the dialysed gold colloid was put on a clean indium–tin-oxide (ITO) glass slide and imaged by a XL30 ESEM FEG SEM operating at 20 kV.

To prepare samples for x-ray diffraction (XRD) measurements, the dialysed gold colloid solution was concentrated, spread on a glass slide and air-dried at room temperature. The XRD pattern was collected on a D/Max 2500 V/PC x-ray diffractometer using Cu Kα (40 kV, 200 mA) radiation.

To investigate the electrochemical properties of the resulting gold nanoparticles, the pH value of the dialysed gold colloid solution was carefully adjusted with 5 mM H_2SO_4 solution until the pH value of the dialysed gold colloid solution was 2–3. Prior to electrochemical experiments, the dialysed gold colloid solution was purged with nitrogen for 15 min. Then the electrochemical experiments were performed at a CHI660 electrochemical workstation (CHI, USA). A conventional three-electrode system was configured, a glassy carbon disc was polished and used as a working electrode (1 mm diameter), with a Ag|AgCl (in a saturated KCl solution) electrode as a reference electrode and a Pt coil as an auxiliary electrode. All the potentials values reported here were referred to the Ag|AgCl (in a saturated KCl solution) electrode.

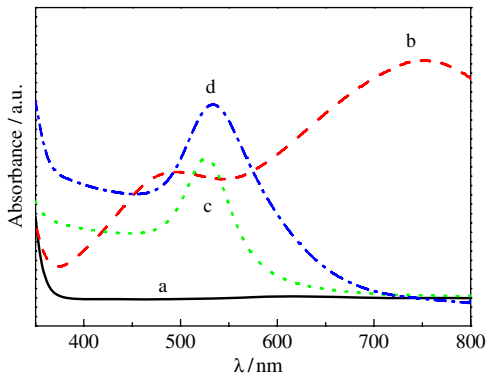

Figure 1. UV–vis spectra of (a) 5 mM PTA, (b) a 5 mM mixture of PTA and AA at pH 5.0, (c) 1 mM $AuCl_4^-$ at 100 °C and (d) 1 mM $AuCl_4^-$ at 20 °C after added such a mixture of PTA and AA.

3. Results and discussion

Polyoxometalates can be reduced in a plethora of ways, for example photochemically [27–29], through ^{60}Co-γ radiolysis [30], electrolytically [31] and with reductants [32]. In this work, L-ascorbic acid and PTA in the aqueous solution with a pH value of 5–6 were mixed. The colour of the solution changed quickly from colourless into dark blue. As shown in figure 1, PTA solution has no obvious absorbance in the range of 400–800 nm. However, when it was mixed with L-ascorbic acid, the UV–vis spectrum of this mixture has an absorption band at 760 nm, which is characteristic of one-electron-reduced polyoxotungstate blue [22, 28], indicating that the PTA was reduced well by L-ascorbic acid. The reduced PTA solution was added into the $HAuCl_4$ solution (prepared at 100 and 20 °C, respectively) under continuous stirring, the solution changed colour from blue into wine red, indicating the formation of Au nanoparticles. The UV–vis spectrum recorded from the PTA–gold solutions showed a sharp absorption band centred at 528 nm (prepared at 100 °C) and at 526 nm (prepared at 20 °C), due to the excitation of surface plasma resonance on the gold nanoparticles. As a mild reductant, L-ascorbic acid has been used in the synthesis of noble metal nanoparticles in the presence of protective reagents [33]. In the absence of phosphotungstic acid, $HAuCl_4$ can also be reduced well by L-ascorbic acid, but the Au colloid is unstable and aggregates quickly. In this study, the PTA–gold solution was extremely stable over time, indicating that the Keggin ion, PTA, was bonded electrostatically and stereochemically to the surface of the Au nanoparticles, and served as a stabilizer for Au nanoparticles.

In this case the chemical synthesis of Au nanoparticles is as shown in scheme 1. The electrons shift from the L-ascorbic acid to PTA, resulting in the reduced PTA, polyoxotungstate blue (step 1 and 2). The reduced PTA transfers electrons to $HAuCl_4$ and finally the Au nanoparticles stabilized by PTA form, as illustrated in scheme 2.

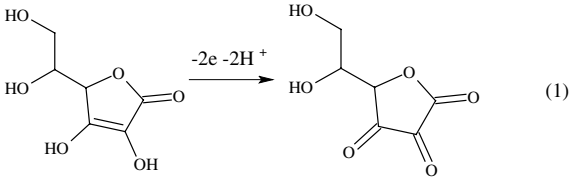

Scheme 1. Description of the redox reaction of L-ascorbic acid, PTA and $AuCl_4^-$.

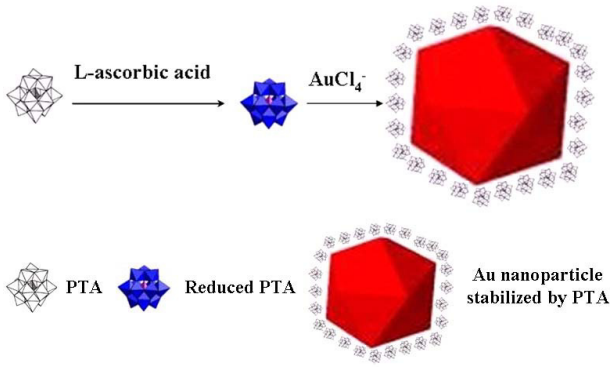

Scheme 2. Illustration of the preparation of Au nanoparticles stabilized by PTA.

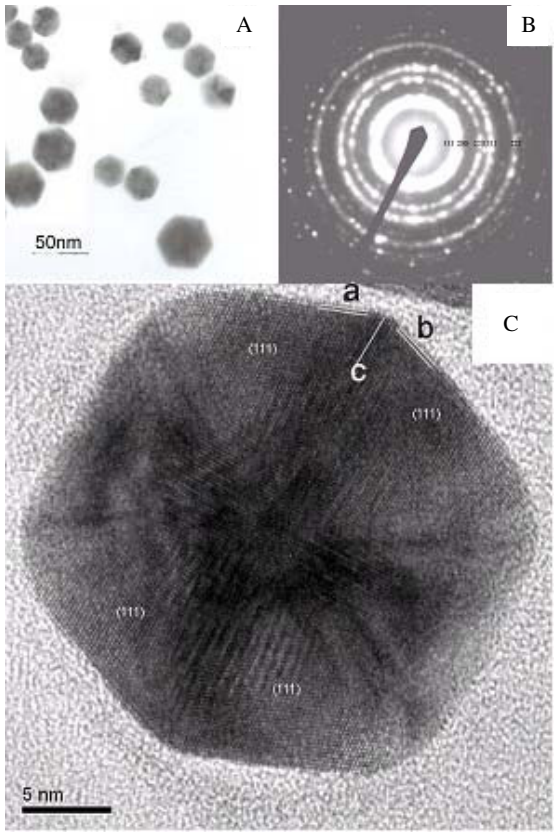

Figure 2. (A) TEM image of hexagonal Au nanoparticles prepared at 100 °C. (B) SAED pattern over several hexagonal Au nanoparticles. (C) High-resolution TEM image of a representative hexagonal Au nanoparticle prepared at 100 °C, and the distribution of (111) facets: (a), (b) are labelled as the *d*-spacing of a (111) facet, and (c) is labelled as a typical twin boundary between (111) facets.

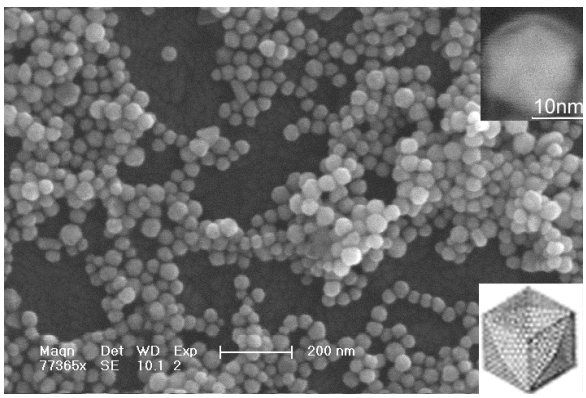

Figure 3. Low-magnification SEM image of polyhedral Au nanoparticles prepared at 100 °C (in the upper inset, an enlarged TEM image shows that the polyhedral Au nanoparticles are icosahedral structures, with a typical geometric icosahedron in the lower inset).

Figure 2(A) shows typical low-magnification TEM images of the gold nanoparticles prepared at 100 °C. The gold nanoparticles are polydispersed and most of them are well-refined hexagons (90%) and pentagons (5%) with sizes ranging from 30 to 50 nm. The size of the particles is defined here as the distance from one edge of hexagonal projection to the opposite one. Figure 2(B) shows the selected-area electron diffraction (SAED) pattern over several Au nanoparticles; it reveals a ring pattern indexed as (111), (200), (220), (311) and (222) of a face-centred cubic (fcc) gold lattice. Figure 2(C) shows a high-resolution TEM image of a hexagonal Au nanoparticle. A multiply twinned boundary at the centre of an Au nanoparticle can be clearly observed from various angles, suggesting the formation of a multiply twinned particle (MTP) which is close to the icosahedral gold nanostructures. The central portion of the TEM image is blurred as a consequence of its sensitivity to misorientation and to distortion of the ideal icosahedron [34]. In addition to the presence of a twin boundary, the Au nanostructure is mainly composed of (111) planes with a *d*-spacing of 0.236 nm (labelled as (a), (b)), and the lattice plane is separated by a twin boundary indicated as a line (labelled as c) on the image.

Further investigation by SEM imaging (in figure 3) shows that the Au nanostructures are mostly polyhedral at low magnification, and the high-magnification image clearly reveals that the Au nanoparticles are icosahedral with a size of 30–50 nm, which is in agreement with the TEM observation. It should be noted that PTA has been used in the synthesis of the spherical Au nanoparticles by photocatalytic reduction [27, 28], which is totally different from our result.

The reaction condition affects the morphology of Au nanocrystals. When Au nanoparticles form at room temperature (20 °C) (as shown in figure 4), they are nearly

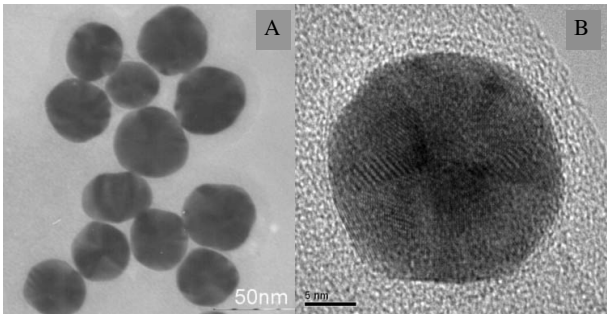

Figure 4. (A) TEM image of spherical Au nanoparticles prepared at 20 °C. (B) High-resolution TEM image of a representative spherical Au nanoparticle prepared at 20 °C.

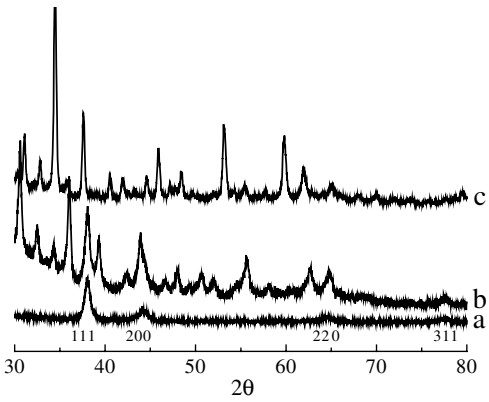

Figure 5. XRD patterns recorded from (A) Au, (B) drop-cast film of PTA–gold colloid solution after dialysis and (C) PTA.

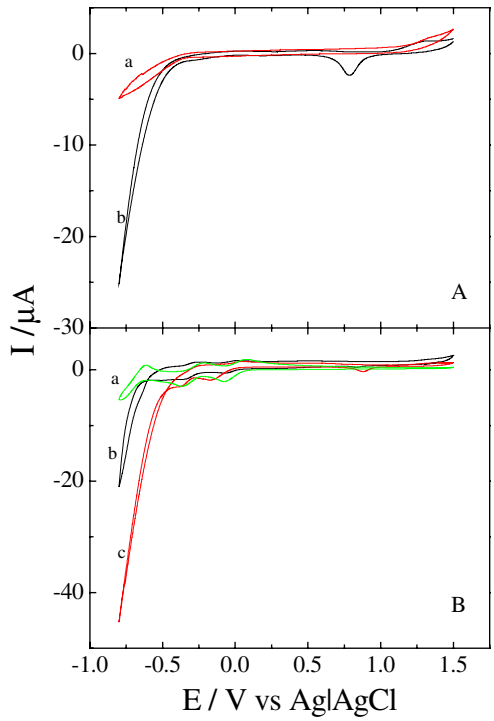

Figure 6. (A) Cyclic voltammograms of bare electrodes: (a) glassy carbon, (b) polycrystalline Au in 5 mM H_2SO_4 solution saturated with N_2 (scan rate: 10 mV s^{-1}). (B) Cyclic voltammograms of bare electrodes: (a) glassy carbon, (c) polycrystalline Au in 5 mM PTA solution saturated with N_2, (b) CV curve in the dialysed PTA–gold colloid solution at a glassy carbon electrode [the pH value of the solution was adjusted to 2–3 by the 5 mM H_2SO_4 (scan rate 10 mV s^{-1})].

spherical with a size distribution of 30–50 nm. A multiply twinned boundary at the centre of the Au nanoparticle can be clearly observed from the high-resolution TEM image, revealing that the nearly spherical Au nanocrystals are also MTPs, but without refined facets. The thermal process may be favourable to the formation of well-refined facets of Au nanocrystals [35]. However, the formation mechanism is still unclear in our investigations.

The presence of Keggin ions in the dialysed PTA–gold colloid solution was examined by the XRD analysis (as shown in figure 5). The Bragg reflection characteristic of fcc gold nanoparticles is identified in this XRD pattern, which is consistent with the SAED result. Besides, the Bragg reflection characteristic of Keggin ions was also present in the XRD pattern, indicating that the Keggin ions are bonded to the surface of gold nanoparticles and serve to stabilize the resulting gold nanoparticles [28].

The electrochemical properties of the Keggin ions were intensively investigated. However, to date, no report has involved the electrochemistry of gold nanoparticle stabilized by PTA.

As is well known, most metal is electrochemically active towards the hydrogen evolution reaction (HER) [36–38]. Figure 6(A) shows that in 5 mM H_2SO_4 solution saturated with N_2, the HER starting potential at the polycrystalline Au electrode (curve b) occurs at about 0.25 V, and a high current output in the hydrogen region (0.25–0.80 V) can be achieved at this electrode, while the glassy carbon electrode (curve a) has no significant response to the HER in the same potential range (0.25–0.80 V).

Figure 6(B) (a and c) shows cyclic voltammograms of the electrode, glassy carbon and polycrystalline Au, in the 5 mM PTA solution saturated with N_2. At the glassy carbon electrode (curve a), it is clear that three reversible well-defined redox curves occur at the formal potential $E_f = 0.0$, -0.30 and -0.7 V, respectively. Here $E_f = (E_a + E_c)/2$, E_a and E_c denote the anodic and cathodic peak potential, respectively. In addition, no significant hydrogen current can be observed from this CV curve. However, a high hydrogen current at 0.8 V can be obtained at the polycrystalline Au electrode, and the HER starts at a potential of about 0.25 V, which is consistent with the results mentioned above for a polycrystalline Au electrode in 5 mM H_2SO_4. The CV curve c of PTA at the polycrystalline Au electrode shows two irreversible redox waves, with $E_f = -0.05$ and -0.30 V, respectively. The last redox wave (in curve c) of PTA at the polycrystalline Au electrode was strikingly deformed due to the HER.

Figure 6(B) (curve b) shows a typical voltammetric response of Au nanoparticles stabilized by PTAs at a glassy carbon electrode. Two redox waves ascribed to redoxidation of the PTA can be clearly seen at $E_f = 0.0$ and 0.03 V, respectively. The peak location is in good accordance with the E_f of PTA at the glassy carbon electrode, which means that the phosphotungstic acid still remains a good Keggin

structure. In addition, the third redox wave (in curve b) of PTA on the surface of Au nanoparticles at the glassy carbon electrode was deformed. As discussed above, the polycrystalline Au is a highly electrochemically active towards HER, but the glassy carbon is not. Thus, this redox wave was ill-defined at glassy carbon as a result of HER in the PTA-stabilized Au nanoparticle solution, which is consistent with the electrochemical properties of PTA at the polycrystalline Au electrode. Differing from the case of PTA at a polycrystalline Au electrode, the HER potential of Au nanoparticles stabilized by PTA bursts is more negative at about 0.55 V.

In summary, we report a one-pot chemical synthesis of highly faceted multiply twinned Au nanocrystals, which was reduced and stabilized by phosphotungstic acid. The Au nanoparticles are of hexagonal shape in TEM and icosahedral in SEM. The gold nanoparticles show electrochemical properties in combination with polyoxometalate and polycrystalline Au—in particular electrochemical activity towards the hydrogen evolution reaction, which might be used further in electrochemical catalysis and the development of chemical sensors.

Acknowledgments

The authors are most grateful to the NSFC, China (no 20475053) and to the Department of Science and Technology of Jilin Province (no 20050102) for their financial support.

References

[1] Taton T A, Mirkin C A and Lestinger R L 2000 Scanometric DNA array detection with nanoparticle probes *Science* **289** 1757

[2] Mucic R C, Storhoff J J, Mirkin C A and Lestinger R L 1989 DNA-directed synthesis of binary nanoparticle network materials *J. Am. Chem. Soc.* **120** 12674

[3] Loweth C J, Caldwell W B, Peng X, Alivisatos A P and Schultz P G 1999 DNA-based assembly of gold nanocrystals *Angew. Chem. Int. Edn* **38** 1808

[4] Pan A, Yang H, Liu R, Yu R, Zou B and Wang Z 2005 Color-tunable photoluminescence of alloyed CdS_xSe_{1-x} nanobelts *J. Am. Chem. Soc.* **127** 15692

[5] Daté M, Okumura M, Tsubota S and Haruta M 2004 Vital role of moisture in the catalytic activity of supported gold nanoparticles *Angew. Chem. Int. Edn* **43** 2129

[6] Mukherjee P, Patra C R, Ghosh A, Kumar R and Sastry M 2002 Characterization and catalytic activity of gold nanoparticles synthesized by autoreduction of aqueous chloroaurate ions with fumed silica *Chem. Mater.* **14** 1678

[7] Chen J *et al* 2005 Gold nanocages: bioconjugation and their potential use as optical imaging contrast agents *Nano. Lett.* **5** 473

[8] Ma Z and Sui S-F 2002 Naked-eye sensitive detection of immunoglobulin G by enlargement of Au nanoparticles in vitro *Angew. Chem. Int. Edn* **41** 2176

[9] Oh E, Hong M-Y, Lee D, Nam S, Yoon H C and Kim H-S 2005 Inhibition assay of biomolecules based on fluorescence resonance energy transfer (FRET) between quantum dots and gold nanoparticles *J. Am. Chem. Soc.* **127** 3270

[10] Katz E and Willner I 2004 Integrated nanoparticle–biomolecule hybrid system: synthesis, properties and applications *Angew. Chem. Int. Edn* **43** 6042

[11] Murphy C J, Sau T K, Gole A M, Orendorff C J, Gao J, Gou L, Hunyadi S E and Li T 2005 Anisotropic metal nanoparticles: synthesis, assembly and optical applications *J. Phys. Chem.* B **109** 13857

[12] Yu Y-Y, Chang S-S, Lee C-L and Wang C R C 1997 Gold nanorods: electrochemical synthesis and optical properties *J. Phys. Chem.* B **101** 6661

[13] Millstone J E, Park S, Shuford K L, Qin L, Schatz G C and Mirkin C A 2005 Observation of a quadrupole plasmon mode for a colloidal solution of gold nanoprisms *J. Am. Chem. Soc.* **127** 5312

[14] Chen S, Wang Z L, Ballato J, Foulger S H and Carroll D L 2003 Monopod, bipod, tripod, and terapod gold nanocrystals *J. Am. Chem. Soc.* **125** 16186

[15] Sun X, Dong S and Wang E 2004 Large-scale synthesis of micro-scale single-crystalline Au plates of nanometer thickness by a wet-chemical route *Angew. Chem. Int. Edn* **43** 6360

[16] Porel S, Singh S and Radhakrishnan T P 2005 Polygonal gold nanoplates in polymer matrix *Chem. Commun.* 2387

[17] Chen Y, Gu X, Nie C-G, Jiang Z-Y, Xie Z-X and Lin C-J 2005 Shape controlled growth of gold nanoparticles by a solution synthesis *Chem. Commun.* 4181

[18] Zhou M, Chen S and Zhao S 2006 Synthesis of icosahedral gold nanocrystals: a thermal process strategy *J. Phys. Chem.* B **110** 4510

[19] Kuo C-H, Chiang T-F, Chen L-J and Huang M H 2004 Synthesis of highly faceted pentagonal- and hexagonal-shaped gold nanoparticles with controlled sizes by sodium dodecyl sulfate *Langmuir* **20** 7820

[20] Kim F, Connor S, Song H, Kuykendall T and Yang P 2004 Platonic gold nanocrystals *Angew. Chem. Int. Edn* **43** 3673

[21] Sau T K and Murphy C J 2004 Room temperature, high-yield synthesis of multiple shapes of gold nanoparticles in aqueous solution *J. Am. Chem. Soc.* **126** 8648

[22] Papaconstantinou E 1989 Photochemistry of polyoxometallates of molybdenum and tungsten and/or vanadium *Chem. Soc. Rev.* **18** 1

[23] Kogan V, Aizenshtat Z, Popovitz-Biro R and Nenmann R 2002 Carbon–carbon and carbon–nitrogen coupling reactions catalyzed by palladium nanoparticles derived from a palladium substituted Keggin-type polyoxometalate *Org. Lett.* **4** 3529

[24] Lin Y and Finke R G 1994 Novel polyoxoanion- and Bu_4N^+-stabilized, isolable, and redissolvable, 20-30 Å $Ir_{\sim 300-900}$ nanoclusters: the kinetically controlled synthesis, characterization, and mechanism of formation of organic solvent-soluble, reproducible size, and reproducible catalytic activity metal nanoclusters *J. Am. Chem. Soc.* **116** 8335

[25] Watzky M A and Finke R G 1997 Transition metal nanocluster formation kinetic and mechanistic studies. A new mechanism when hydrogen is the reductant: slow, continuous nucleation and fast autocatalytic surface growth *J. Am. Chem. Soc.* **119** 10382

[26] Aiken J D and Finke R G 1999 Polyoxoanion-and tetrabutylammonium- stabilized $Rh(0)_n$ nanoclusters: unprecedented nanocluster catalytic lifetime in solution *J. Am. Chem. Soc.* **121** 8803

[27] Troupis A, Hiskia A and Papaconstantinou E 2002 Synthesis of metal nanoparticles by using polyoxometalates as photocatalysts and stabilizers *Angew. Chem. Int. Edn* **41** 1911

[28] Mandal S, Selvakannan P R, Pasricha R and Sastry M 2003 Keggin ions as UV-switchable reducing agents in the synthesis of Au core–Ag shell nanoparticles *J. Am. Chem. Soc.* **125** 8440

[29] Yamase T 1998 Photo- and electrochromism of polyoxometalates and related materials *Chem. Rev.* **98** 307

[30] Papaconstantinou E 1982 Relative electron-donating ability of simple alcohol radicals toward 12-heteropolytungstates. A pulse radiolysis study *J. Chem. Soc. Faraday. Trans.* 1 **78** 2769

[31] Weinstock I A 1998 Homogeneous-phase electron-transfer reactions of polyoxometalates *Chem. Rev.* **98** 113
[32] Müller A, Shah S Q N and Schmidtmann H B M 1999 Molecular growth from a Mo_{176} to a Mo_{248} cluster *Nature* **397** 48
[33] Yamamoto M, Kashiwagi Y, Sakata T, Mori H and Nakamoto M 2005 Synthesis and morphology of star-shaped gold nanoplates protected by poly(*N*-vinyl-2-pyrrolidone) *Chem. Mater.* **17** 5391
[34] Buffat P-Á, Flüeli M, Spycher R, Stadelmann P and Borel J-P 1991 Crystallographic structure of small gold particles studied by high-resolution electron microscopy *Faraday Discuss.* **92** 173
[35] Jin R, Egusa S and Scherer N F 2004 Thermally-induced formation of atomic AU clusters and conversion into nanocubes *J. Am. Chem. Soc.* **126** 9900
[36] Markovic N M, Grgur B N and Ross P N 1997 Temperature-dependent hydrogen electrochemistry on platinum low-index single-crystal surfaces in acid solutions *J. Phys. Chem.* B **101** 5405
[37] Perez J, Gonzalez E R and Villullas H 1998 Hydrogen evolution reaction on gold single-crystal electrodes in acid solutions *J. Phys. Chem.* B **102** 10931
[38] Hamelin A, Stoicoviciu L, Chang S-C and Weaver M J 1991 Temperature dependence of proton electroreduction kinetics at gold(111) and (210) surfaces and annealing of surface defects *J. Electroanal. Chem.* **307** 183